Piezoelectric semiconductor acoustic cavities

G. Rozas,[1] M. F. Pascual Winter,[1] A. Fainstein,[1,*] B. Jusserand,[2] P. O. Vaccaro,[3] S. Saravanan,[3] and N. Saito[3]
[1]*Centro Atómico Bariloche & Instituto Balseiro, C.N.E.A., 8400 S. C. de Bariloche, R. N., Argentina*
[2]*Institut des Nanosciences de Paris, UMR CNRS 7588, Université Pierre et Marie Curie, Campus Boucicaut, 140 Rue de Lourmel, 75015 Paris, France*
[3]*ATR Wave Engineering Laboratories, 2-2-2 Hikaridai, Keihanna Science City, Kyoto 619-0288, Japan*
(Received 10 March 2005; revised manuscript received 29 April 2005; published 14 July 2005)

We describe semiconductor cavities based on strained $Ga_{0.85}In_{0.15}As/AlAs$ multilayers with permanent built-in piezoelectric fields that confine acoustic phonons in the THz range. The possible role of piezoelectric fields on the phonon lifetimes and on Raman scattering is discussed. Phonon mirrors and cavities grown along [001] (non-piezoelectric) and along [311] (piezoelectric) are studied and compared using high-resolution Raman spectra and photoelastic model calculations. The high quality of the grown [001]([311]) structures is demonstrated by the observation of up to 7(5) orders of folded acoustic phonons and the excellent agreement with theory. We observe a large broadening of the acoustic phonon peaks in the piezoelectric [311] structures upon carrier injection with near-gap excitation. Such acoustic phonon lifetime reduction evidences a strongly modified electron-acoustic phonon interaction in these structures.

DOI: 10.1103/PhysRevB.72.035331 PACS number(s): 78.30.Fs, 63.20.Dj, 78.66.Fd, 42.60.Da

Planar acoustic cavities have been recently introduced as resonant structures that confine acoustic vibrations in the GHz-THz range.[1] Drawing a parallel with optical microcavities,[2] one can foresee the possibility of using such cavities to modify the way in which sound interacts with light,[3] with other phonons,[4] and with electrons. They could, in addition, provide the feedback mechanism required for phonon "lasing" devices.[5] In this paper we will focus our attention on the possibility of tailoring the electron-phonon interaction in acoustic cavities. In fact, the amplified and localized strain associated to the acoustic confined mode should enhance this coupling. However, the deformation potential interaction that couples acoustic phonons and electrons is relatively small, and thus a sizable effect due to the confinement is not to be expected unless large strains are attained. On the other hand, the situation should be qualitatively different for piezoelectric materials in which strain plays an essentially different role.[6,7] In these materials, besides the deformation potential coupling, a potentially much stronger Fröhlich-like interaction with carriers is present. We thus propose here acoustic cavities with built-in piezoelectric fields as potential devices with an enhanced electron-acoustic phonon coupling and, consequently, an amplified sound-light interaction.

Exploiting the piezoelectric coupling between acoustic phonons and photons in superlattices (SL's), a new type of polariton has been recently proposed to exist in ferroelectric oxide multilayers due to the retarded interaction between light and the transverse polarization accompanying longitudinal acoustic waves in these materials.[8] Polar III-V semiconductors do not possess inversion symmetry and are intrinsically piezoelectric materials. When these materials are grown in multilayers with lattice mismatch, the induced strain may lead to *permanent* built-in electric fields along the growth direction. In fact, it turns out that in structures grown along [001] the existence of piezoelectric fields is forbidden by symmetry.[9] On the other hand, the latter are present for almost any other growth direction, and very large fields (larger than 10^5 V cm^{-1}) have been observed in such cases in a variety of III-V multilayers.[9] The presence of these *permanent* strain-induced fields modifies the potential landscape sensed by carriers, changing in a fundamental way the optical properties of these structures. What we want to emphasize here is an aspect that has been, to the best of our knowledge, largely overlooked. This is the modification introduced by strain-induced piezoelectric fields on the coupling between acoustic phonons and electrons, and through it on the phonon and electron dephasing, and on the inelastic scattering of acoustic phonons by light.

Let us first discuss the electron-acoustic phonon coupling in SL's from a qualitative point of view. We show in Fig. 1 a scheme of the top and bottom of the valence and conduction bands, respectively, of SL's without (a) and with (b) built-in piezoelectric fields, and their variation upon deformation by acoustic phonon induced strain. In the standard case (a), by deforming the structure the phonons modify the energy levels of the quantum wells, leading to the relatively weak so-called deformation potential interaction.[10] This mechanism

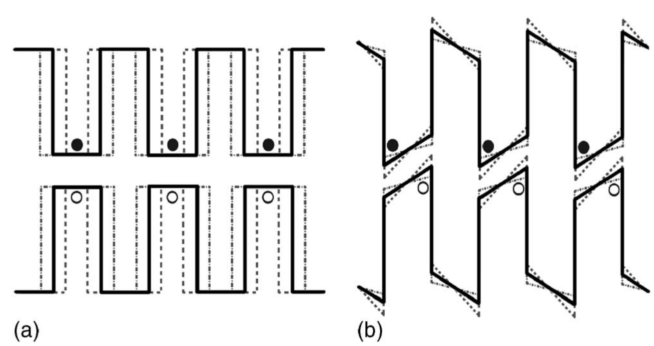

FIG. 1. The scheme of SL electronic bands (solid lines) without (a) and with (b) built-in piezoelectric fields. The dashed and dashed-dotted lines represent their variation upon deformation by acoustic phonon induced strain. The solid and empty circles indicate light-generated electron-hole pairs.

adds to the bulk-like deformation potential coupling also present in SL's.[11] When a piezoelectric field is present (b), an acoustic phonon of the appropriate wavelength will modulate the strain in such a way that the spatial periodicity of the modulated component of the built-in field (typically in the GHz-THz range) will match the periodic distribution of the permanent one. This modulation of polarization fields leads to an additional interaction mechanism between the acoustic-phonons and the electrons that is similar to the Fröhlich coupling between the latter and longitudinal optic (LO) phonons.[11] In principle, if this coupling is with carriers it can lead to an additional dephasing mechanism.[12,13] On the other hand, if the phonon modulation affects *virtual* electronic levels that are intermediate states for a light-matter interaction, an amplified high-frequency modulation of the dielectric function and consequently of the inelastically (Raman) scattered light is to be expected. The electric-field-induced Raman cross section is even on the electric field E, and thus proportional to E^2.[14] Thus, we can infer that in a piezoelectric SL a new contribution to the Raman signal should exist that is proportional to $E_{pz}\delta E_{pz}$, where E_{pz} and δE_{pz} are, respectively, the permanent piezoelectric field along the growth direction z and its modulation by the acoustic phonon strain. In view of the huge fields present in semiconductor SL's (10^5-10^6 V cm^{-1}), a strongly modified Raman interaction should exist. We note that Raman processes have a counterpart in the time domain corresponding to coherent phonon generation. This corresponds to the impulsive generation of in-phase vibrations after a short and intense laser pulse (typically in the ps and fs range). Interestingly, huge coherent phonon generation efficiency in GaInN/GaN piezoelectric SL's has been reported.[6,7] The proposed mechanism, i.e., the screening of the piezoelectric built-in field by photoexcited carriers, is one of the aspects of the modified electron-acoustic-phonon interaction we are addressing here.[6,7]

It is the purpose of this paper to investigate these effects in strained phonon mirrors and cavities with and without induced permanent piezoelectric fields. For this purpose we have chosen to work with $Ga_{0.85}In_{0.15}As/AlAs$ SL's for three reasons. Firstly, these materials have been largely studied and the sample growth with molecular beam epitaxy (MBE) techniques is well managed with atomic layer control. Secondly, they are known to display piezoelectric fields in excess of 10^5 V cm^{-1} with In concentrations around 15% for which good epitaxial growth is achieved.[9] And, thirdly, AlAs barriers allow for the confinement of electronic states, thus enabling the resonant excitation of carriers specifically in the $Ga_{0.85}In_{0.15}As$ wells.

Phonon mirrors are basically SL's made of two materials with contrasting acoustic impedance.[15] Such structures reflect sound only within limited regions around a wavelength λ (and frequencies that are multiple of $v/2\lambda$, with v an effective sound velocity), which is set by design. These high reflectance regions are called "stop-bands." At the center of the Brillouin zone the lowest energy phonon stop-band is optimized by using ($\lambda/4, 3\lambda/4$) stacks,[3,16] that is, a period equal to an acoustic phonon wavelength. This stop-band corresponds to the first minigap at the Brillouin zone center in an acoustic folded-phonon scheme.[16] Two such mirrors enclosing a spacer of thickness equal to an integer number of half-wavelengths defines a planar cavity.[1,3] The phonon velocities and Raman selection rules for [311] GaAs/AlAs SL's have been worked out in detail as a function of the corresponding elastic constants and densities by Popovic and co-workers.[17,18] Those for [001] structures are, on the other hand, well established. For the latter case two degenerate transverse acoustic (TA, Raman forbidden in backscattering configuration) and one longitudinal acoustic (LA, Raman allowed in backscattering) branches exist. For [311] grown structures three nondegenerate bands exist, being one purely transverse (TA), another quasi-transverse (QTA), and the third quasi-longitudinal (QLA). All three modes are Raman allowed (though with different selection rules) in backscattering (BS) geometry.[17]

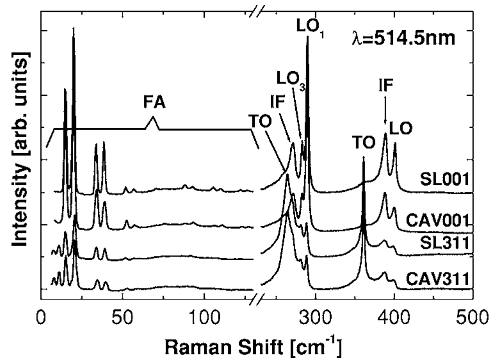

FIG. 2. The phonon mirror (SL) and cavity (CAV) room temperature Raman spectra taken with incident and scattered polarizations parallel to a [110] axis ([001] growth direction) and a [$\bar{2}$33] axis ([311]), using 514.5 nm excitation and the spectrometer in subtractive mode. Both the folded acoustic (FA) phonon (0–130 cm^{-1}) and optic phonon (250–500 cm^{-1}) spectral regions are shown. LO, TO, IF, and LO_3 stand for longitudinal, transverse, interface, and confined optic phonon modes, respectively.

We report data on four different samples: two phonon mirrors (grown along [001], SL001, and along [311], SL311) and two phonon cavities (grown along [001], CAV001, and along [311], CAV311). The 24-period mirrors are designed to have an optimized first minigap stop-band and reflectivity ($R\sim 0.997$).[3] The first Brillouin zone-center minigap and the cavity modes were nominally set at $\sim$18 cm^{-1}. The cavities, on the other hand, consist of two 12-period mirrors enclosing a $\lambda/2$ spacer (nominal finesse $\sim$330). Thus, the latter can be basically understood as a phononic defect in an otherwise periodic SL identical to the phonon mirrors. The layer thicknesses of the $Ga_{0.85}In_{0.15}As/AlAs$ [001]([311]) mirrors were 21 Å/78 Å(23 Å/84 Å), while the [001]([311]) $Ga_{0.85}In_{0.15}As$ cavity spacer was 42(46) Å thick. The reported Raman experiments were collected at room temperature and at 80 K using as exciting radiation different visible lines of an Ar-Kr ion laser focussed on a 20 μm spot. The collected spectra were dispersed using both subtractive (lower resolution) and additive (higher resolution) configurations of a Jobin-Yvon triple spectrometer and detected with a liquid N_2-cooled charge coupled device (CCD).[4]

Figure 2 displays room temperature Raman spectra, taken with incident and scattered polarizations parallel to a [$\bar{2}$33] axis, for the [311] structures, and parallel to [110] for the

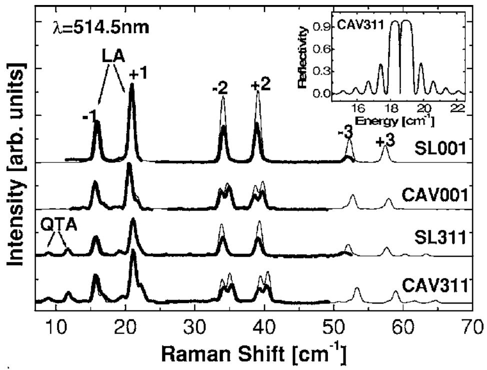

FIG. 3. The room temperature acoustic phonon Raman spectra obtained with an additive high-resolution configuration (thick solid curves). The thin solid curves correspond to spectra calculated with a photoelastic model. LA and QTA label longitudinal and quasi-transverse acoustic modes, respectively. The numbers indicate the successive orders of the LA folded phonon pairs. Inset: acoustic reflectivity calculated for the [311] cavity using the structural parameters deduced from the Raman scattering data. Note the high-Q cavity mode with zero reflectivity within the acoustic stop-band.

[001] grown samples. For these experiments we used 30 mW of 514.5 nm excitation and the spectrometer in subtractive mode. Both the folded acoustic (FA) phonon ($0-130$ cm^{-1}) and optic phonon ($250-500$ cm^{-1}) spectral regions are shown. The latter is characterized by two separate series of peaks. Those at $250-300$ cm^{-1} correspond to GaAs-like vibrations of the $Ga_{0.85}In_{0.15}As$ layers, while the peaks at $350-400$ cm^{-1} are the AlAs vibrations of the barriers. The spectra agree well with the Raman selection rules for [001] and [311] grown SL's, which predict respectively the observation of only LO, and both LO and TO (transverse optic) modes.[18] Besides these characteristic peaks, intense interface-like (IF) and GaAs confined phonon (LO_3) modes are also observed. As regards the FA spectral region, note the unusually large number of replicas (up to seven for [001] and up to five for [311]). This reflects the excellent quality of the structures. In agreement with theory, only LA modes are observed along [001], while both QLA and QTA modes appear for polarized backscattering along [311].[17]

The acoustic and optic phonon spectra presented above clearly distinguish between [001] and [311] grown structures. However, within the standard resolution of the subtractive mode of the triple Raman setup no difference can be identified between the phonon mirrors (SL's) and the cavity structures. The situation is completely different when an additive higher resolution configuration is used, as shown for the acoustic modes with thick solid curves in Fig. 3. In this figure also Raman spectra calculated with a photoelastic model[4] are displayed with thin solid curves. The phonon displacements were calculated using a matrix method implementation of a continuum model that includes zero-strain boundary conditions at the SL-air interface.[4] In addition, the curves were Gaussian convoluted to take into account the experimental resolution. The experimental curves, on the other hand, were corrected for the Bose factor. Several features should be highlighted from these spectra. (*i*) There is an excellent agreement with theory. The only adjusted parameters were the exact SL's period (which differed from the nominal values in $\leqslant 3\%$), the cavity-spacer thickness (which was increased by $\sim 2\%$), and the intensity ratio between QLA and QTA modes for the [311] structures. (*ii*) The SL spectra display the usual symmetric peaks corresponding either to LA modes ([001]) or to QLA and QTA modes ([311]). The shoulder of the +1 component of the first FA pair in SL311 corresponds to the second-order (+2) component of the QTA mode. (*iii*) The cavity spectra, on the other hand, display splittings of the FA pairs that are quite precisely taken into account in the model calculations.[19] This splitting shows up as a high energy shoulder in the first-order component, and as a clear almost symmetric doubling for the second-order pair. In fact, the line shape is quite sensitive to the cavity spacer thickness, and can be used to characterize the phonon resonator even if the cavity confined mode is not observable in BS geometry.[4] The direct observation of the cavity mode requires, on the other hand, access to a forward scattering geometry.[1]

The excellent agreement between experiment and theory in Fig. 3 can be taken as an experimental demonstration of a high-quality piezoelectric cavity based on strained III-V semiconductors grown on high-index substrates. An example of the acoustic reflectivity calculated for the [311] cavity using the parameters deduced from the above presented Raman data is shown as an inset on Fig. 3. According to our calculations, for the reported [311] cavity the elastic displacement at the spacer is enhanced by a factor of ~ 6, implying an increase of ~ 40 in the deformation energy resonant in the cavity as compared to a standard SL without acoustic confinement. These numbers increase to ~ 20 and ~ 400, respectively, by using 20-period mirrors instead of 12. What needs then to be determined is the role of the piezoelectric fields in the coupling between acoustic phonons and electrons or light in these structures. Effects of piezoelectric fields on Raman scattering by *optic* phonons in $Ga_{0.85}In_{0.15}As/AlAs$ SL's have been previously reported by Sela and co-workers.[20] These experiments display selection rule modifications and LO phonon scattering enhancement upon resonant excitation with the spin-orbit-split $E_0+\Delta_0$ band. For our samples with relatively thin $Ga_{0.85}In_{0.15}As$ quantum wells (21 Å) and strong AlAs barrier confinement, resonant experiments tuned to the $E_0+\Delta_0$ band or to the $Ga_{0.85}In_{0.15}As$ quantum well confined states would require tunable dye lasers in the $1.7-2.1$ eV ($\sim 590-720$ nm) range. Photoluminescence measurements show that at 80 K the E_0 gap of the phonon mirror SL's falls around 720 nm (~ 1.727 eV), while the $E_0+\Delta_0$ is estimated to be at ~ 590 nm (~ 2.09 eV).

In Fig. 4 we report Raman data, excited with 5 mW of the red 647.1 nm line of our Ar-Kr ion laser. These show that, in fact, significant changes occur when the Raman acoustic phonon peaks of the [311] grown structures are excited close to resonance. Note that the [001] sample spectra are essentially equivalent to those in Fig. 2, taken with the green 514.5 nm laser line. On the other hand, the peaks for the piezoelectric [311] structures strongly broaden (at least a factor of 3 at 647.1 nm) and shift with respect to the [001] structures. This contrasting behavior becomes more evident

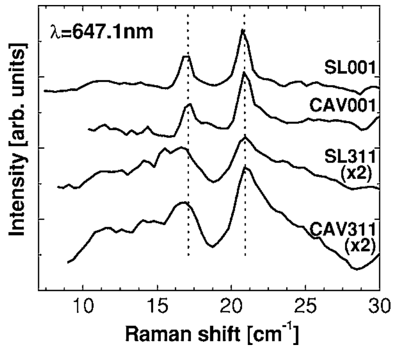

FIG. 4. The Raman spectra of SL's and cavity (CAV) structures grown both along [001] and [311], and excited at 80 K with 5 mW of the red 647.1 nm line of an Ar—Kr ion laser. Note the large broadening and shift of the acoustic phonon peaks of the [311] structures. The vertical dashed lines are only guides to the eye.

when Raman spectra for the [001] and [311] structures taken with different discrete wavelengths from the Ar-Kr laser are compared. This is shown for the [001] and [311] SL's in Fig. 5. The Raman intensities have been corrected for the grating and detector response of the spectrometer. In addition, for ease of comparison the spectra have been scaled to similar amplitudes by multiplication with the number shown between brackets. Narrow folded phonon doublets are observed for all wavelengths in the [001] SL. The scattered intensity increases towards the red because of the expected resonant enhancement of the spectra.[11] The only relevant feature that calls the attention is the appearance at 676 nm (close to resonance with the E_0 gap) of other peak and dip-like features (note, e.g., the dip-like feature observed at $\sim 28\ \mathrm{cm}^{-1}$). The latter could be due to scattering of acoustic phonons at the Brillouin zone edge due to wave vector nonconservation as described in detail for resonant Raman scattering by T. Ruf and co-workers.[21] To more clearly display the folded phonon peaks for 676 nm in Fig. 5 a strong background that could

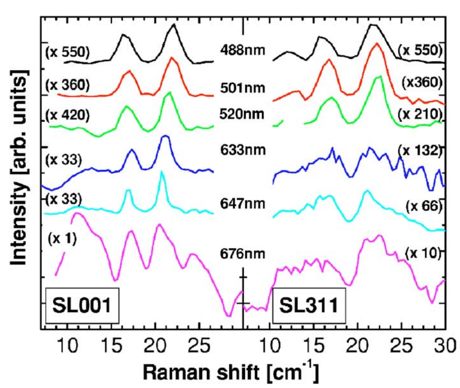

FIG. 5. (Color online) The Raman spectra of SL structures grown both along [001] (left) and [311] (right), excited at 80 K with 5 mW of various laser lines of an Ar-Kr ion laser. The Raman intensities have been corrected for the grating and detector response of the spectrometer. In addition, the spectra have been scaled by multiplication with the number between brackets. Note the acoustic folded phonon line broadening and amplitude reduction in the case of near-resonant (red) excitation for the [311] SL. See text for details.

also have the same origin (as explained in Ref. 21) was subtracted from the data. On the other hand, for the [311] SL striking effects occur when the laser excitation is in the red region of the spectra, either with 632.8, 647.1, or 676 nm. In these cases, and contrasting with the higher energy spectra, the folded-phonon peaks clearly broaden and reduce their amplitude. This is particularly noteworthy for 632.8 nm, which is close to the $E_0+\Delta_0$ $Ga_{0.85}In_{0.15}As$ well gap, and at 676 nm, which is close to the E_0 gap. In the latter case, an approximately tenfold amplitude reduction is observed with respect to the [001] SL spectra taken under identical conditions. Raman investigations with a tunable laser would be desirable to fully characterize the resonant behavior. In any case, what is clearly and systematically observed for near-resonant excitation is a relative broadening and amplitude reduction of the folded acoustic phonon peaks for the [311] structures with built-in piezoelectric fields.

To the best of our knowledge, little theoretical work has been reported describing the acoustic phonons, their Fröhlich-like interaction with electrons, and their scattering with light in piezoelectric strained SL's. Sanders *et al.* and Chern *et al.*[22] have presented a thorough analysis of the coherent phonon generation process due to ultra-fast laser impulsions in SL's with piezoelectric fields. Nevertheless, we are not aware of any theoretical work addressing the Raman scattering by acoustic phonons in similar structures. On the other hand, very recently it has been pointed out the existence of an electron-acoustic-phonon coupling mechanism associated with the dependence of crystal dielectric permittivity on the strain (the so-called Pekar mechanism),[12,13] which could play a major role in electron relaxation in nanostructures characterized by strong confining electric fields.[23] We believe that a theory incorporating such kind of electron-phonon coupling could provide a formal framework to understand the phenomena we report here. In fact, the presented results can be understood at least qualitatively as due to a strong coupling between the electron-hole pairs excited close to resonance with the red laser light, and the polarization carrying piezoelectric acoustic phonons. The picture is similar to what is well known to occur between LO phonons and electrons or electron-hole pairs in polar doped or photoexcited semiconductors, respectively.[24,25] In this case, the LO phonon is strongly screened upon carrier injection, leading to line broadenings and energy shifts. Depending on the excitations dispersion and damping, this coupling can lead in addition to coupled plasmon-phonon modes. As significant line broadening and amplitude reduction only occur for [311] samples we conclude that for the experiments we report in Figs. 4 and 5 the phenomena is mainly governed by an additional carrier-induced acoustic phonon dephasing (and hence a line-broadening) that involves the piezoelectric fields. The details of this strongly enhanced interaction should become clearer with complete resonant experiments as those performed for optic phonons by Sela and co-workers.[20] In addition, we believe that strong insight could be attained by time-dependent transmission measurements using femtosecond pump and probe setups as reported for GaInN/GaN SL's in Ref. 6. In such experiments both the photoexcitation screening of the piezoelectric fields and the strong phonon confinement should lead to efficient monoenergetic coherent phonon generation.

In conclusion, we have discussed the role of strain-induced piezoelectric fields in SL's on the coupling between acoustic phonons and charge. We have proposed piezoelectric acoustic cavities with built-in electric fields designed to have an enhanced electron-phonon and photon-phonon coupling. These structures exploit the added effect of a Fröhlich-like interaction of polarization modulating acoustic phonons and their confinement in a resonating structure. These concepts have been demonstrated in structures of excellent quality based on strained $Ga_{0.85}In_{0.15}As/AlAs$ multilayers grown along [311]. High-resolution Raman scattering results clearly evidence the acoustic phonons of phonon mirror and cavity structures. These results compare excellently with photoelastic model calculations of the Raman efficiency, providing a precise tool for the characterization of these acoustic devices. Upon almost resonant excitation of carriers in the $Ga_{0.85}In_{0.15}As$ quantum wells we observe a large broadening of the acoustic phonon peaks as compared to similar non-piezoelectric [001] $Ga_{0.85}In_{0.15}As/AlAs$ structures. These results evidence the existence of a strong electron-acoustic phonon coupling in the piezoelectric mirrors and cavities, similar to that existent for LO phonons in polar materials.

Support from SECyT-ECOS is acknowledged. AF acknowledges support from the ONR (USA), and PV, SS and NS from the National Institute of Information and Communications Technology of Japan.

*Email address: afains@cab.cnea.gov.ar

[1] M. Trigo, A. Bruchhausen, A. Fainstein, B. Jusserand, and V. Thierry-Mieg, Phys. Rev. Lett. **89**, 227402 (2002).

[2] *Confined Electrons and Photons: New Physics and Applications*, edited by E. Burstein and C. Weisbuch, (Plenum, New York, 1995).

[3] P. Lacharmoise, A. Fainstein, B. Jusserand, and V. Thierry-Mieg, Appl. Phys. Lett. **84**, 3274 (2004).

[4] M. F. Pascual Winter, A. Fainstein, M. Trigo, T. Eckhause, R. Merlin, A. Cho, and J. Chen, Phys. Rev. B **71**, 085305 (2005).

[5] P. A. Fokker, J. I. Dijkhuis, and H. W. de Wijn, Phys. Rev. B **55**, 2925 (1997); see also I. Camps, S. S. Makler, H. M. Pastawski, and L. E. F. Foa Torres, Phys. Rev. B **64**, 125311 (2001), and references therein.

[6] C.-K. Sun, J.-C. Liang, and X.-Y. Yu, Phys. Rev. Lett. **84**, 179 (2000).

[7] Ümit Özgür, Chang-Won Lee, and Henry O. Everitt, Phys. Rev. Lett. **86**, 5604 (2001).

[8] Y. Y. Zhu, X. J. Zhang, Y. Q. Lu, Y. F. Chen, S. N. Zhu, and N. B. Ming, Phys. Rev. Lett. **90**, 053903 (2003).

[9] L. De Caro and L. Tapfer, Phys. Rev. B **51**, 4374 (1995).

[10] F. T. Vasko and V. V. Mitin, Phys. Rev. B **52**, 1500 (1995); P. A. Knipp and T. L. Reinecke, *ibid.* **52**, 5923 (1995).

[11] P. Y. Yu and M. Cardona, *Fundamentals of Semiconductors: Physics and Material Properties* (Springer, Berlin, 2003).

[12] A. A. Demidenko, V. N. Piskovoi, S. I. Pekar, and B. E. Tsekvava, Zh. Eksp. Teor. Fiz. **50**, 124 (1966) [Sov. Phys. JETP **23**, 84 (1966)].

[13] Y. V. Gulyaev, Fiz. Tverd. Tela (Leningrad) **9**, 1816 (1967) [Sov. Phys. Solid State **9**, 1425 (1967)].

[14] M. Kuball, N. Esser, T. Ruf, C. Ulrich, M. Cardona, K. Eberl, A. Garcia-Cristobal, and A. Cantarero, Phys. Rev. B **51**, 7353 (1995).

[15] P. V. Santos, L. Ley, J. Mebert, and O. Koblinger, Phys. Rev. B **36**, 4858 (1987).

[16] B. Jusserand and M. Cardona, in *Light Scattering in Solids V*, edited by M. Cardona and G. Güntherodt (Springer, Heidelberg, 1989), p. 49.

[17] Z. V. Popovic, J. Spitzer, T. Ruf, M. Cardona, R. Notzel, and K. Ploog, Phys. Rev. B **48**, 1659 (1993).

[18] Z. V. Popovic, E. Richter, J. Spitzer, M. Cardona, A. J. Shields, R. Notzel, and K. Ploog, Phys. Rev. B **49**, 7577 (1994).

[19] M. Giehler, T. Ruf, M. Cardona, and K. Ploog, Phys. Rev. B **55**, 7124 (1997).

[20] I. Sela, D. L. Smith, S. Subbanna, and H. Kroemer, Phys. Rev. B **46**, 1480 (1992).

[21] See, for example, T. Ruf, J. Spitzer, V. F. Sapega, V. I. Belitsky, M. Cardona, and K. Ploog, Phys. Rev. B **50**, 1792 (1994) and references therein.

[22] G. D. Sanders, C. J. Stanton, and C. S. Kim, Phys. Rev. B **64**, 235316 (2001); **66**, 079903 (2002); see also G.-W. Chern, K.-H. Lin, and C.-K. Sun, J. Appl. Phys. **95**, 1114 (2004).

[23] B. A. Glavin, V. A. Kochelap, T. L. Linnik, and K. W. Kim, Phys. Rev. B **71**, 081305(R) (2005).

[24] G. Abstreiter, M. Cardona, and A. Pinczuk, in *Light Scattering in Solids IV*, edited by M. Cardona and G. Güntherodt (Springer, Berlin, 1984).

[25] A. Pinczuk, J. Shah, and P. A. Wolff, Phys. Rev. Lett. **47**, 1487 (1981).